Diffusion properties of time-resolved trajectories in the wake behind a cylinder

Ali Rahimi Khojasteh, Dominique Heitz

HAL Id: hal-03864735

https://hal.inrae.fr/hal-03864735

Submitted on 21 Nov 2022

Diffusion properties of time-resolved trajectories in the wake behind a cylinder

AR. Khojasteh[1,*], D. Heitz[1]

1:INRAE, OPAALE, 17 avenue de Cucillé, 35044, Rennes, France
*Corresponding author: ali.rahimi-khojasteh@inrae.fr

Keywords: Lagrangian statistics, 4D-PTV, Second-order structure function

ABSTRACT

We investigate the computation of the Lagrangian second-order structure-function for describing the multiscale dynamics of turbulence based on measured particle trajectory data. Using time-resolved three-dimensional particle tracking velocimetry (4D-PTV), we statistically quantified turbulent properties of the anisotropic and inhomogeneous flow field behind a cylinder at a Reynolds number of 3900. Lagrangian statistical analysis has been performed on nearly 12000 trajectories for 4000 time steps.

1. Introduction

Recent advances in time-resolved three-dimensional particle tracking velocimetry (4D-PTV) extend the possibility of exploring the Lagrangian viewpoint of turbulent properties along particle trajectories. The recent work of Viggiano et al. (2021) showed how we could obtain fundamental Lagrangian turbulence quantities, particularly the Lagrangian structure function scaling constant C_0, from anisotropic and inhomogeneous dynamics of a jet flow by normalising the trajectories based on local Eulerian scales. The C_0 constant in the Lagrangian framework is in a similar role as the Kolmogorov constant in the Eulerian framework (Viggiano et al., 2021). In the present study, we are interested in examining the stationarisation process proposed by Viggiano et al. (2021) in the wake behind a smooth cylinder and studying Lagrangian statistics from Spatio-temporal trajectories.

2. Lagrangian diffusion properties

Taylor's turbulent diffusion theory (Taylor, 1922) has been used widely to study homogeneous isotropic turbulent (HIT) flows. In a given time τ, Taylor's theory computes the Lagrangian two-point correlation function $R_{uu}^L(\tau)$ for an ensemble of particle trajectories based on the mean square displacements of particles $\sigma^2(\tau)$ that can be written as,
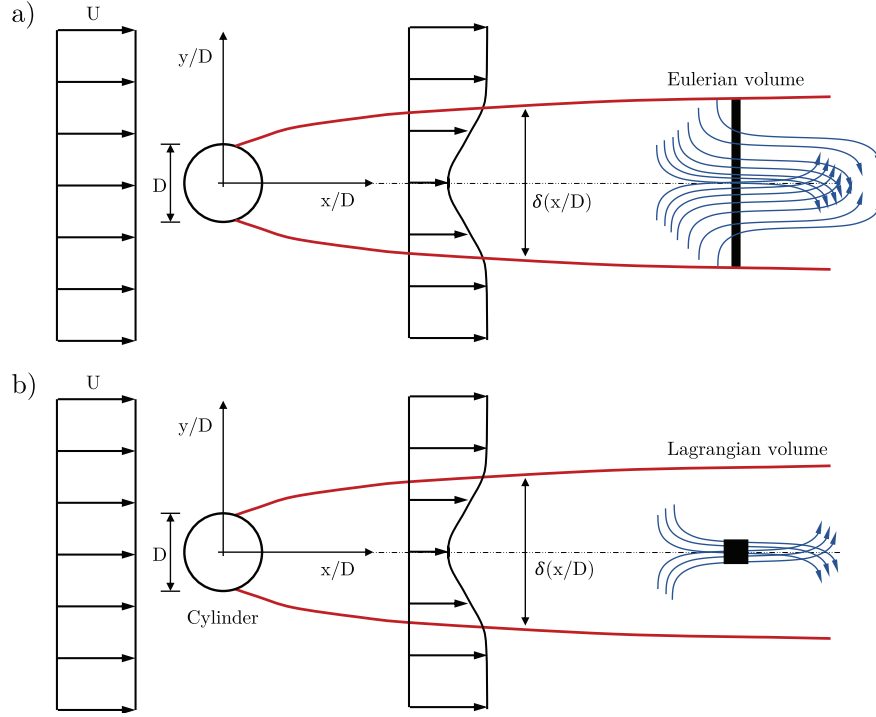
Figure 1. Computation of the wake flow statistics from Lagrangian trajectories. (a) Eulerian statistics at a certain downstream x/D over all trajectories passing the Eulerian volume. (b) Lagrangian statistics at a certain downstream x/D over all trajectories passing the Lagrangian volume.

$$\frac{\mathrm{d}^2 \sigma^2}{\mathrm{d}\tau^2}(\tau) = 2R_{uu}^L(\tau) \tag{1}$$

The turbulent diffusion process to Lagrangian statistical properties of particle trajectories can be linked if we assume that particles in the present study act as a tracer (Viggiano et al., 2021). This means that all the inertial effects are neglected, and particles perfectly follow the flow motion. Therefore, we can compute the Lagrangian second-order structure-function as,

$$S_2^L(\tau) = \langle [u(t+\tau) - u(t)]^2 \rangle = 2\left(r_{uu}^L(0) - R_{uu}^L(\tau)\right), \tag{2}$$

where the Lagrangian trajectories were obtained from three-dimensional particle tracking velocimetry (4D-PTV). Therefore, we can compute the Lagrangian universal constant C_0 for the Lagrangian second-order structure function. This constant was found to be strongly sensitive to the Reynolds number, large-scale anisotropy and inhomogeneity of flow (Viggiano et al., 2021). This means that computation of the C_0 constant is complicated in anisotropic and inhomogeneous turbulent cases. In the wake behind a cylinder, turbulent length and time scales evolve as flow goes downstream, creating non-stationary anisotropic and inhomogeneous dynamics. Batchelor's diffusion theory (Batchelor, 1957) as an extension of Taylor's theory, proposed using the Lagrangian stationarisation idea for inhomogeneous cases such as the wake flow. Stationarisation is a process based on Eulerian self-similarity properties that stationaries the Lagrangian dynamics. Recently, Viggiano et al. (2021) investigated the highly anisotropic and inhomogeneous case in a free shear turbulent jet.
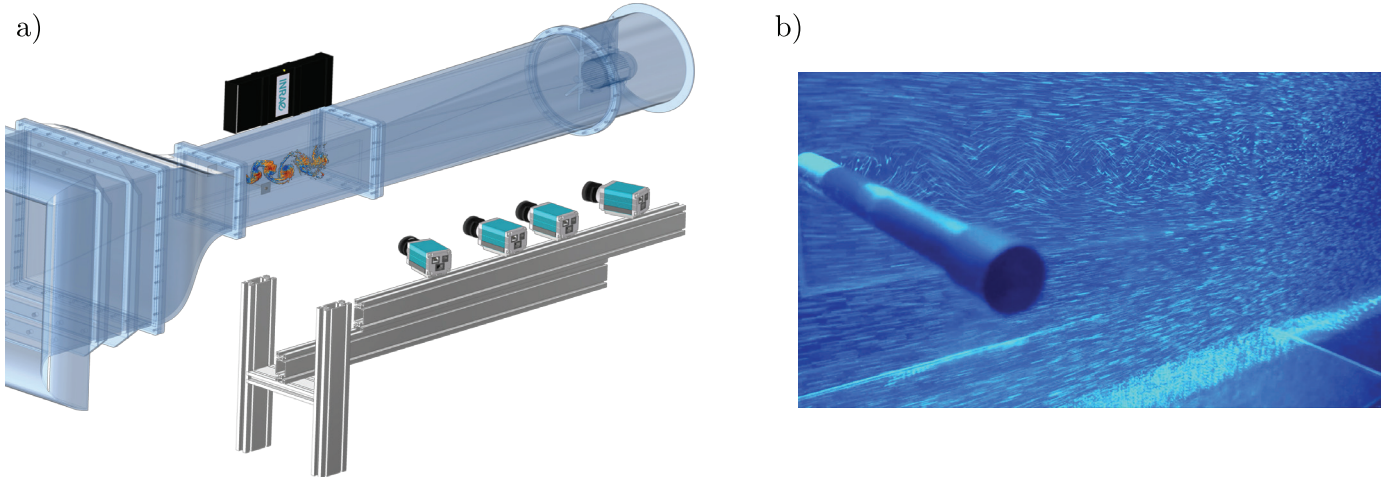
a)

b)

Figure 2. Experiment setup design for the cylinder wake flow at Reynolds 9m66 (a) Schematic of the camera setup design. (b) One snapshot of HFSB tracer particles passing downstream of the cylinder.

Viggiano et al. (2021) characterised the inertial-range dynamics and the Lagrangian universal constant C_0 by the Lagrangian stationarisation idea. Two Lagrangian second-order structure function and two-point correlation function statistics needs to be computed. The Lagrangian second-order structure function can be written as,

$$S_2^L(\tau) = \langle [u(t+\tau) - u(t)]^2 \rangle = C_0 \frac{\varepsilon_i \tau}{\sigma_{u_i}^2},$$ (3)

where   is the turbulent energy dissipation. To stationarise the Lagrangian in-stationarity of the wake flow, as proposed by Viggiano et al. (2021), we compute the Eulerian mean velocity by fine-scale reconstruction (VIC# Jeon et al. (2018)) from Lagrangian trajectories. Then the deviation between the instantaneous and the mean components non-dimensionalised by the Reynolds stress terms is as follows,

$$\tilde{u}_i(\tau) = \frac{u_i(\tau) - \bar{u}_i(x(\tau))}{\sigma_{u_i}(x(\tau))}.$$ (4)

We can achieve a stationarised flow field with non-dimensionalised fluctuations through the entire spatial domain for every time step. With the same derivation spirit discussed in Viggiano et al. (2021); Ouellette (2021), we are interested in exploring Lagrangian properties for the wake behind a cylinder. We will characterise the Eulerian/Lagrangian turbulent properties as well as self-similarity behaviour, followed by estimation of the Lagrangian universal constant C_0.

3. 4D-PTVe xperiments etup

An experimental study of the cylinder wake flow at Reynolds number equal to 3900 (same value as the synthetic data) was performed. Experiments were carried out in the wind tunnel equipped
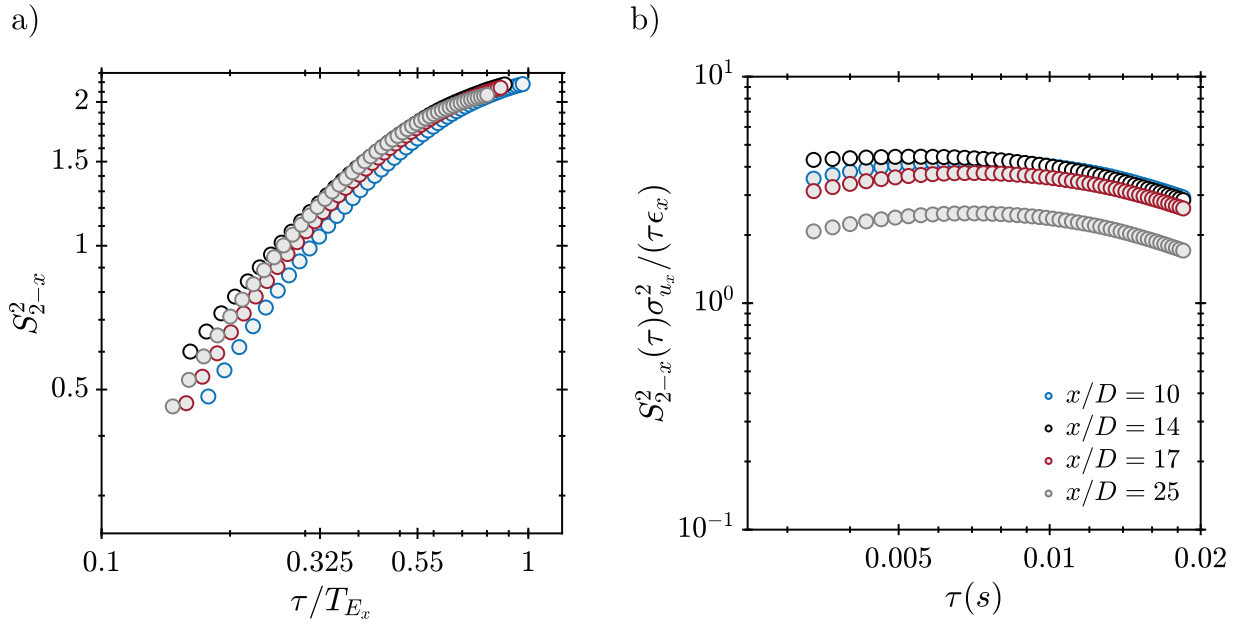
a)

b)

Figure 3. Lagrangian second order structure function of the streamwise direction at four downstream locations. (a) Non-dimensional $S_{2,x}^L$ as a function of non-dimensional timescale. (b) Re-dimensionalised structure function representing the C_0 constant.

with a centrifugal fan, a diffuser, a plenum chamber with honeycomb and grids, a contraction section decreasing by 4, and an area with transparent walls for testing. With the aid of hot wire anemometry, the velocity profile at the wind tunnel entrance was checked to ensure uniformity. The free-stream turbulence intensity level was found to be less than 0.2%. The cross-section of the testing zone is square, with a width of $28\,\mathrm{cm}$ and a length of $100\,\mathrm{cm}$. It has a slightly tilted upper wall to reduce longitudinal pressure gradients. It is possible to choose a continuous flow velocity of to $8\,\mathrm{m/s}$.

In this classic wake flow case, the complexity of the flow topology is captured by preserving the areas where turbulence is produced. There are three such regions on an obstacle: the boundary layer, the two shear layers at the limit of the recirculation region, and the wake. We designed an experimental setup with four cameras as shown in Figure 2.a. Four CMOS SpeedSense DANTEC cameras with a resolution of $1280{\times}800$ pixels and the maximum frequency of 3 kHz are empowered. Cameras are equipped with Nikon 105 mm lenses. The calibration error was lower than 0.06 pixel and reduced to 0.04 after the volume self-calibration. We captured roughly $10D$ to $25D$ downstream of the cylinder for the present study. The acquisition was long enough to observe dynamic evolutions of the von Kármán vortex streets downstream of the cylinder. Details of the experimental setup can be found in Khojasteh et al. (2021).

◀

Table 1. Eulerian parameters for various x/D positions.

x/D	σ_{u_x} $(\mathrm{m\ s^{-1}})$	ε_z $(\mathrm{W\ kg^{-1}})$	η_z $(\mu\mathrm{m})$	τ_{η_z} (ms)	λ_z $(\mu\mathrm{m})$	Re_λ	L_{E_z} (mm)	T_{E_z} (ms)
9	0.31	3.33	17.65	2.1	255.2	53.97	60.7	19.39
11	0.30	3.15	17.90	2.2	255.3	52.54	61	20.02
14	0.29	2.83	18.38	2.3	258.8	51.15	61.9	21.16
17	0.28	2.56	18.85	2.4	267.1	51.81	62.1	21.65
19	0.27	2.40	19.16	2.5	267.8	50.40	62.7	22.52
22	0.26	2.15	19.70	2.6	273.6	49.78	62.9	23.34
25	0.26	2.31	19.33	2.5	266.9	49.21	62.9	23.04

4. Wake flow statistics

The velocity component of each trajectory was computed after fitting a curve over noisy reconstructed positions. The Eulerian fields were computed using fine-scale reconstruction (VIC# Jeon et al. (2018)) between trajectories to achieve gridded velocity fields. Thereafter, time-averaged mean $\bar{u}_i\,(x(\tau))$ and Reynolds stress $\sigma_{u_i}\,(x(\tau))$ terms can be computed by averaging all instantaneous Eulerian velocity fields to start the process in equation (4). Schematic of the wake flow self similar behaviour downstream of the cylinder is shown in figure 1. Due to the loss of momentum cases by the cylinder, the wake velocities are smaller than the free stream region. The wake thickness increases as the flow travels downstream of the cylinder. We can compute the Eulerian statistics within the area of the wake. Ensemble of all trajectories passing a virtual volume inside the wake at a certain x/D is considered to achieve statistically converged Eulerian properties as shown in figure 1. The Eulerian volume has the dimension of $\delta\,(x/D) \times 2D$ in y and z directions with $0.5\,\mathrm{mm}$ depth in direction as suggested by Viggiano et al. Viggiano et al. (2021). Therefore, we can compute the Eulerian second order structure function over the ensemble of spatial velocity increments of each pair trajectories passing the Eulerian volume. Velocity components were stationarised with equation (4). We computed the Eulerian turbulent properties in seven downstream positions varying from $x/D = 9$ to 25 as listed in table 1. Nearly constant values of the Taylor microscale Re_λ shows that the stationarisation process suggested by Batchelor Batchelor (1957) is valid for the self similar wake flow far downstream of the wake flow. Decay of the dissipation rate ε_{u_x} toward downstream is also in with power-law decay in self-similar flows. Both Kolmogorov η_x, and integral L_{E_x} length scales are growing as flow goes far downstream.

The evolution of Eulerian dissipation rate ε_{u_x}, Kolmogorov length scale η_x, and integral scale T_{E_x} will be used to compute Lagrangian statistical properties. To compute the Lagrangian second order statistics, we assume a small cube volume inside the wake with the length of $\delta(x/D)/3$ (suggested

by Viggiano et al. Viggiano et al. (2021)) and index all trajectories passing the volume. Following equation (3), we compute temporal velocity increments on each individual trajectory. The ensemble of computed temporal increments is then averaged to compute the Lagrangian second order structure function. By solving the left side of equation (3), we can compute the C_0 constant where ε_i and $\sigma_{u_i}^2$ are the Eulerian dissipation rate and the averaged velocity standard deviation over the Lagrangian volume.

The Lagrangian second order structure function at four downstream locations is plotted in figure 3. The result of non-dimensional $S_{2,x}^2$ in far downstream shows that the Lagrangian statistics becomes independent of the downstream position ($x/D > 10$). In the present study, we were unable to reach converged statistics for $x/D < 10$. We also observe that the non-dimensional $S_{2,x}^2$ has linear relation with τ where $\eta_x < \tau < T_{E_x}$. These findings are in agreement with the free jet self-similar case Viggiano et al. (2021).

5. Conclusion

Lagrangian statistics of the wake flow experiment showed that the Lagrangian statistics becomes independent of the downstream position $x/D > 10$ (see figure 3) illustrating self-similar behaviour of the wake. These findings are in agreement with the free jet self-similar case (Viggiano et al. (2021)). Figure 3.b suggests the C_0 value, which should stay nearly constant in the inertial range. C_0 is found to be between $2 - 4$ for the selected downstream locations. Based on the study by Sawford Sawford (1991), C_0 should be around 2.6 for the corresponding Taylor microscale Reynolds number. Therefore, the estimated C_0 of the present study is in the same order as Sawford's model.

References

Batchelor, G. K. (1957). Diffusion in free turbulent shear flows. *Journal of Fluid Mechanics*, *3*(1), 67–80. doi: 10.1017/S0022112057000488

Jeon, Y. J., Schneiders, J. F., Müller, M., Michaelis, D., & Wieneke, B. (2018). 4D flow field reconstruction from particle tracks by VIC+ with additional constraints and multigrid approximation. *18th International Symposium on Flow Visualization*.

Khojasteh, A. R., Heitz, D., Yang, Y., & Fiabane, L. (2021). Particle position prediction based on Lagrangian coherency for flow over a cylinder in 4D-PTV. In *14th international symposium on particle image velocimetry* (pp. 1–9). Illinois, USA.

Ouellette, N. T. (2021). Extending the reach of Lagrangian analysis in turbulence. *Journal of Fluid Mechanics*, *924*, 1. doi: 10.1017/jfm.2021.493

Sawford, B. L. (1991). Reynolds number effects in Lagrangian stochastic models of turbulent dispersion. *Physics of Fluids A*, *3*(6), 1577–1586. doi: 10.1063/1.857937

Taylor, G. I. (1922, 1). Diffusion by continuous movements. *Proceedings of the London Mathematical Society*, *s2-20*(1), 196–212. doi: 10.1112/plms/s2-20.1.196

Viggiano, B., Basset, T., Solovitz, S., Barois, T., Gibert, M., Mordant, N., … Cal, R. B. (2021). Lagrangian diffusion properties of a free shear turbulent jet. *Journal of Fluid Mechanics*, *918*, 25. doi: 10.1017/jfm.2021.325